Optical manifestations of symmetry breaking in bilayer graphene

D. S. L. Abergel

Condensed Matter Theory Center, Department of Physics, University of Maryland, College Park, Maryland 20742, USA

Vladimir I. Fal'ko

Department of Physics, Lancaster University, Lancaster LA1 4YB, United Kingdom
(Received 4 May 2012; published 31 July 2012)

We propose a spectroscopic method of identifying broken symmetry states of bilayer graphene. We demonstrate theoretically that, in contrast to gapped states, a strained bilayer crystal or nematic phase of the electronic liquid are distinguishable by the dependence of the line shape of absorption on the polarization of the light. This property is characteristic for both the infrared and far-infrared spectral ranges, which correspond to the absorption by transitions between low-energy bands and split bands, and transitions between the low-energy valence and conduction bands, respectively.

In this Rapid Communication we study how symmetry breaking in bilayer graphene (BLG)[1] manifests itself in the optical spectra in the infrared (IR) and far-infrared (FIR) spectral ranges.[2–9] Symmetry breaking in BLG may be caused both by external perturbations and by internally developed instabilities generated by the electron-electron interactions. For example, strain in BLG which might be inflicted on the crystal involuntarily upon thermal annealing and cooling of suspended BLG devices would asymmetrically change the topology of the low-energy dispersion.[10–12] Also, by applying a perpendicular electric field, one breaks the inversion symmetry of the lattice opening an externally tunable gap between the valence and conduction bands.[1] Alternatively, at low temperatures, undoped pristine BLG may undergo a spontaneous symmetry-breaking transition into one of the recently discussed strongly correlated ground states.[13–23] In particular, the phases favored by the renormalization of short-range electron-electron interaction constants[22–24] are a nematic state in which the isotropy of the band structure is reduced in a similar way to strained BLG,[10,25] and gapped layer-antiferromagnetic[20] and spin flux phases.[24] Although several transport experiments[25–28] reported observations of some broken symmetry states in BLG, the exact nature of the ground state still remains to be established.

Here, we show how infrared (IR) and far-infrared (FIR) absorption spectroscopy can be used to distinguish between some of the broken symmetries. The feature discussed below is that strain (or a phase transition to the nematic state) induces a dependence of absorption of light on the polarization of the radiation. This anisotropy can be characterized by a factor

$$Q = \frac{g_\parallel - g_\perp}{g_\parallel + g_\perp}, \qquad (1)$$

where $g_\parallel$ ($g_\perp$) is the absorption coefficient of light with linear polarization **e** parallel (perpendicular) to the principal strain axis (or the direction chosen by the order parameter of the nematic phase). In contrast, the gapped phases show isotropic absorption and notable qualitative differences in the line shape of their absorption spectrum as compared to the strained (nematic) and unperturbed BLG states.

The absorption coefficient[2,3] analyzed in this study,

$$g_{\mathbf{e}}(\omega) = \frac{4\pi\hbar g_s}{c\omega\mathcal{A}} \text{Im} \sum_{\substack{\mathbf{p},\lambda,\lambda' \\ \alpha,\beta}} \frac{f(\mathbf{p}\lambda') - f(\mathbf{p}\lambda)}{\omega + \epsilon_{\mathbf{p}\lambda} - \epsilon_{\mathbf{p}\lambda'} + i0} e_\alpha M_{\alpha\beta}^{\lambda\lambda'} e_\beta^*,$$
$$(2)$$

is given by the ratio of the Joule heating and the flux of incident radiation. Equation (2) describes transitions between initial and final plane wave states marked by indices λ which include the band, branch, and valley (spin is also taken into account); $\epsilon_{\mathbf{p}\lambda}$ is the energy of a plane wave with momentum **p**, f is the Fermi function, $\mathcal{A}$ is the normalization area, and

$$M_{\alpha\beta}^{\lambda\lambda'} = \langle \mathbf{p}\lambda | \hat{j}_\alpha^\dagger | \mathbf{p}\lambda' \rangle \langle \mathbf{p}\lambda' | \hat{j}_\beta | \mathbf{p}\lambda \rangle \qquad (3)$$

are determined by the current density operator $\hat{\mathbf{j}} = e\partial_{\mathbf{p}}\mathcal{H}$. Since the momentum transferred by light is negligibly small, in $M_{\alpha\beta}^{\lambda\lambda'}$ the momenta of electrons in the initial and final states of the interband transitions are taken to be equal. The corresponding plane wave state wave functions are the four-component eigenstates $|\cdots\rangle \propto (\psi_{A_1}, \xi\psi_{B_2}, \psi_{A_2}, \xi\psi_{B_1})$ of the Hamiltonian[1,10]

$$\mathcal{H} = \begin{pmatrix} 0 & v\boldsymbol{\sigma} \cdot \mathbf{p} \\ v\boldsymbol{\sigma} \cdot \mathbf{p} & \gamma_1 \sigma_x \tau_z \end{pmatrix} + \delta H, \qquad (4)$$

where $A_{1(2)}$ and $B_{1(2)}$ identify the sublattices of the honeycomb lattices in the top (bottom) layers, $\xi = \pm$ distinguishes the K and K' corners of the hexagonal Brillouin zone, and Pauli matrices σ_x, σ_y, σ_z, and τ_z act on the sublattice and valley components of $|\cdots\rangle$, respectively. Also, γ_1 stands for the interlayer coupling between atoms on A_2 and B_1 lattice sites, and v is the Dirac velocity for monolayer graphene.

For unperturbed BLG ($\delta H = 0$), Eq. (4) determines[1] a pair of low-energy bands near the Brillouin zone corners with spectrum $\epsilon_{\mathbf{p}\pm} = \pm p^2/2m^* \equiv \pm\epsilon_0$, $m^* = \gamma_1/2v^2 \approx 0.035 m_e$ for states located mainly on sublattices A_1 and B_2. Equation (4) also determines two split bands with quadratic dispersion $\epsilon_{\mathbf{p}\pm} \approx \pm(\gamma_1 + \epsilon_0)$ and wave functions that have equal weight on lattices A_2 and B_1. Note that the split band states are almost unperturbed by the strain or the formation of a nematic phase or one of the gapped phases.[1]

For the sake of convenience, the "valley momentum" $\mathbf{p}$ in Eqs. (3) and (4) is determined with respect to the position of the Dirac point in the graphene monolayer, which is shifted from the Brillouin zone corners K and K' in a homogeneously strained crystal.[29] In monolayer graphene, such a shift $\mathbf{p} \rightarrow \mathbf{p}' + \mathbf{a} \equiv \mathbf{p}$ in the momentum space is trivially absorbed into a gauge transformation so that it does not influence observable characteristics, such as the absorption spectrum. In contrast, in BLG the interplay of such a shift and the interlayer skew hopping γ_3 which couples sublattices A_1 and B_2 generates a perturbation which cannot be eliminated from the Hamiltonian by any gauge transformation. This, as well as other possible symmetry-breaking perturbations in BLG are included in

$$\delta H = \begin{cases} w\tau_z \boldsymbol{\sigma} \cdot \boldsymbol{\Lambda}, & \text{strain/nematic (Refs. 10 and 22–24),} \\ u\tau_z \sigma_z, & \text{layer asymm. (Refs. 1, 16, and 17),} \\ u(\mathbf{s} \cdot \mathbf{S})\tau_z \sigma_z, & \text{antiferro. (Refs. 19–21 and 24),} \\ u(\mathbf{s} \cdot \mathbf{S})\sigma_z & \text{spin flux (Ref. 24).} \end{cases}$$

The first term in δH accounts for the effect of strain[30] or nematic order, with the direction of the unit vector $\boldsymbol{\Lambda} = (\cos 2\theta, \sin 2\theta)$ set by the direction $\boldsymbol{\ell} = (\cos \theta, \sin \theta)$ of the principal stretching direction. This perturbation changes the low-energy electron dispersion into

$$\epsilon_{\mathbf{p}\pm} = \pm\frac{1}{2m}|\mathbf{p} - \sqrt{2mw}\boldsymbol{\ell}| \times |\mathbf{p} + \sqrt{2mw}\boldsymbol{\ell}|, \quad (5)$$

which features a Lifshitz transition at $\epsilon = \pm|w|$, from an almost parabolic dispersion at $|\epsilon| \gg |w|$ to a pair of Dirac cones at $\mathbf{p} = \pm\sqrt{2mw}\boldsymbol{\ell}$ shifted from each other along the anisotropy axis $\boldsymbol{\ell}$. In the following, the axis $\boldsymbol{\ell}$ will be used as the reference direction to distinguish between "parallel," $\mathbf{e} \parallel \boldsymbol{\ell}$, and "perpendicular," $\mathbf{e} \perp \boldsymbol{\ell}$, polarizations of light and the corresponding absorption coefficients $g_\parallel$ and $g_\perp$ in Eq. (1).

Also, in δH, antiferromagnetic (AF) and spin-flux (SF) states are characterized by a splitting $2u$ between the valence and conduction bands at the K point and have identical spectra $\epsilon_{\mathbf{p}\pm} = \pm\sqrt{u^2 + \epsilon_0^2}$, the same as in graphene with an asymmetry gap opened, for example, by a perpendicular electric field.[1] For magnetic phases of BLG, $\mathbf{S}$ characterizes the spin quantization axis, but since the current operator $\hat{\mathbf{j}}$ does not depend on the spin at all, these BLG states will behave identically in the optical absorption.

In the IR spectral range, $\omega \approx \gamma_1 \approx 0.4$ eV, where ω is the energy of the incident light, the optical transitions which are sensitive to the BLG symmetry breaking are those between the small momentum parts of the split bands and the low-energy bands. In addition, the spectral density of IR absorption includes the contribution from the transitions between the two low-energy bands at high momentum which provides an almost-constant background in the absorption spectrum.[2,3] In Fig. 1(a) we show the calculated absorption spectrum for the two characteristic polarizations of light and the polarization factor Q for undoped, strained BLG with $w = 5$ meV at $T = 3$ K. The absorption spectrum of BLG in the nematic phase would have the same features: The anisotropy of the
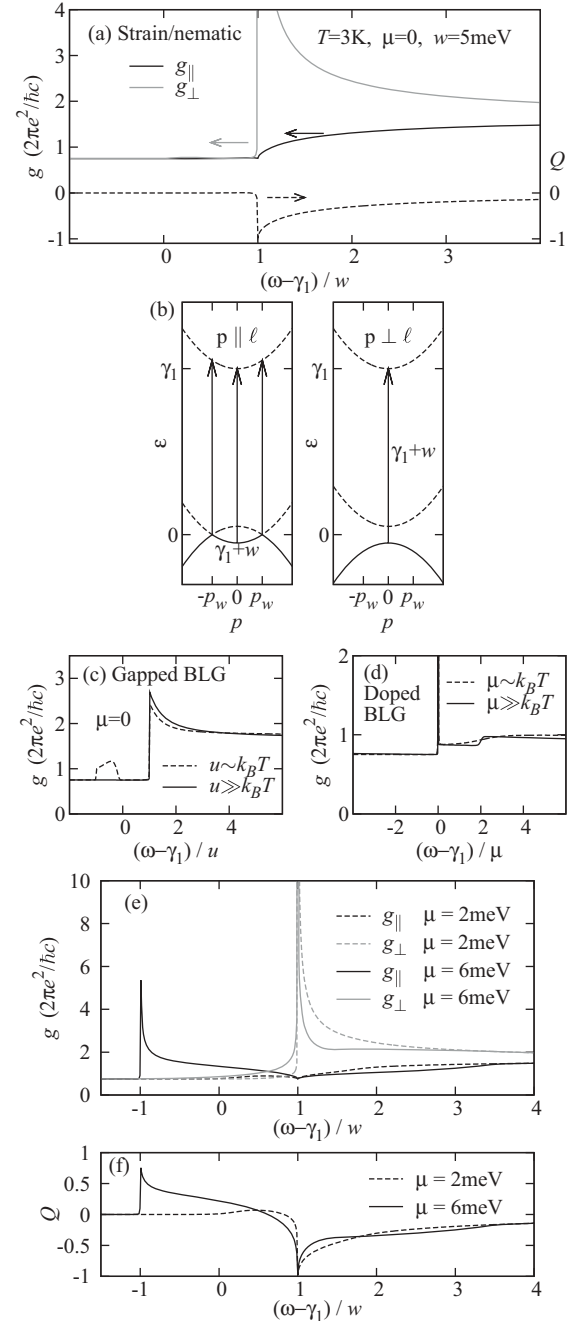

FIG. 1. (a) Absorption coefficients $g_\parallel$ and $g_\perp$ and absorption anisotropy Q for undoped strained/nematic bilayer graphene with $w = 5$ meV and $T = 3$ K. (b) Sketch illustrating optical transitions from the low-energy bands at $\mu = 0$ and $T = 0$ in strained BLG or the nematic phase of BLG. Solid (dashed) lines denote filled (empty) states. The two extremal parts of the dispersion are shown for $\mathbf{p} \parallel \boldsymbol{\ell}$ (with Dirac points at $\pm p_w$ with $p_w = \sqrt{2mw}$), and $\mathbf{p} \perp \boldsymbol{\ell}$. The arrows mark the range of p for which the threshold transitions with $\omega = \gamma_1 + w$ exist. (c) The absorption coefficient for undoped, gapped bilayer graphene. (d) The absorption coefficient for the unperturbed system with finite chemical potential μ. (e) Absorption coefficient and (f) anisotropy Q of strained BLG with finite doping for $w = 5$ meV and $T = 3$ K, for $\mu = 2$ meV $< w$ and $\mu = 6$ meV $> w$.

absorption for $\omega \approx \gamma_1 + w$, where the absorption for $\mathbf{e} \perp \boldsymbol{\ell}$ (gray line) shows a strong peak near the threshold whereas

absorption for $\mathbf{e} \parallel \boldsymbol{\ell}$ (black line) is weak:

$$g_\perp \propto (\omega - \gamma_1 - w)^{-2}, \quad g_\parallel \to 0.$$

This occurs because the matrix elements M in Eq. (3) preferentially select transitions with $\mathbf{p} \perp \boldsymbol{\ell}$ for $g_\parallel$ and $\mathbf{p} \parallel \boldsymbol{\ell}$ for $g_\perp$. In the first case, when $\mathbf{p} \perp \boldsymbol{\ell}$, only transitions from right at the center of the K point have the threshold energy $\gamma_1 + w$, but in contrast, when $\mathbf{p} \parallel \boldsymbol{\ell}$, there is a finite range of momenta, $-\sqrt{2mw} < p < \sqrt{2mw}$, where the low-energy valence band and conduction split band are shifted on the energy scale by exactly $\gamma_1 + w$ [Fig. 1(b)]. (This is also true for the valence split band and the low-energy conduction band.) This produces a singularity at the interband absorption edge, $\gamma_1 + w$.[31]

For comparison, in Fig. 1(c) we show the absorption spectrum characteristic for any of the gapped states of BLG. Here, the absorption coefficient does not depend on the polarization of the photon and there is a feature at the threshold $\omega = \gamma_1 + u$ of the lowest-energy interband transitions. The height of this peak is constant for $u \gg k_B T$. When $k_B T \gtrsim u$ (this situation is considered having in mind the gapped state caused by the interlayer asymmetry due to external perturbation rather than an intrinsic phase transition) thermal occupation of the low-energy conduction band also allows transitions to the split band with energy $\gamma_1 - u$, which yields a small additional polarization-independent peak in $g(\omega)$. The absorption of IR light by unperturbed BLG with finite doping and chemical potential μ is shown in Fig. 1(d),[32] in precise agreement with previous calculations of the optical conductivity.[2,3,33]

Figure 1(e) shows the absorption spectrum of strained BLG with finite doping (the chemical potential $\mu \neq 0$ is counted from the Dirac point energy). Note that the nematic phase is not expected to survive at finite doping. When $|\mu| < w$ (dashed line), the absorption spectrum remains almost unchanged as compared to the undoped case, but for $|\mu| > w$ (solid line) a new peak appears at $\omega = \gamma_1 - w$ in the $\mathbf{e} \parallel \boldsymbol{\ell}$ polarization but not in the $\mathbf{e} \perp \boldsymbol{\ell}$ polarization. This occurs because, with this level of doping, transitions from the low-energy conduction band above the Lifshitz transition become accessible. This asymmetry manifests itself in the polarization degree Q of the absorption, shown in Fig. 1(f) for $|\mu| < w$ (dashed line) and $|\mu| > w$ (solid line).

We now turn our attention to absorption in the FIR frequency range, $|\omega| \sim 2w \ll \gamma_1$, where the relevant optical transitions occur between the two low-energy bands. Figure 2(a) illustrates features of the absorption by strained BLG for the two characteristic polarizations of FIR radiation, $\mathbf{e} \parallel \boldsymbol{\ell}$ and $\mathbf{e} \perp \boldsymbol{\ell}$: a weak polarization dependence described by $Q \approx +0.3$ at energies $\omega \approx 2w$, indicating that the absorption is strongest for light polarized in the direction of the principal strain axis. Note that for FIR light the relation between absorption in different polarizations is opposite to what we found for the IR spectral range. A dip in the absorption at very low energies is due to the finite temperature. The absorption by strained BLG with finite doping is shown in Fig. 2(b). The only effect of the doping is to cut off the absorption for $\omega < |\mu|$. The absorption by the gapped phase is shown in Fig. 2(c) for comparison: It has no polarization dependence but has a peak at $\omega = 2u$ corresponding to the threshold of the optical transition. For the doped but unperturbed BLG, Fig. 2(d) shows a step in $g(\omega)$ at $\omega = 2\mu$.[3] Therefore, one can distinguish the type of
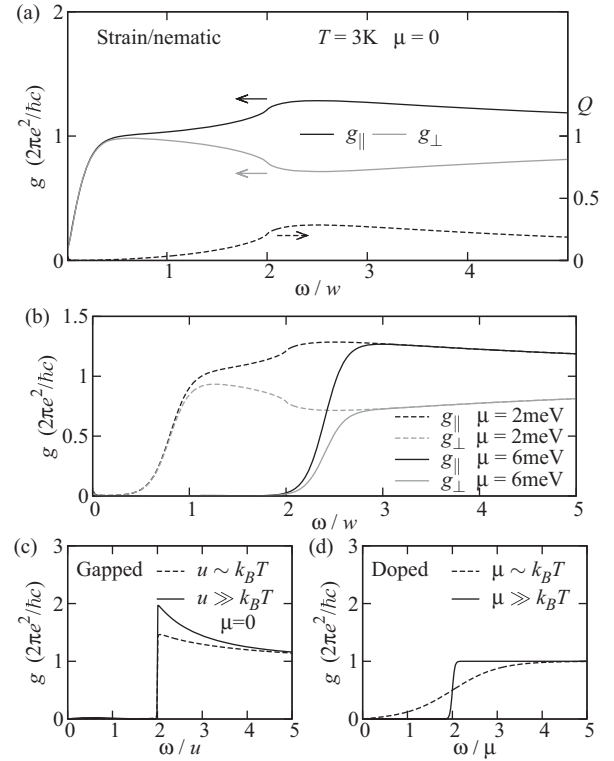

FIG. 2. Absorption coefficient in the FIR frequency range for (a) undoped strained BLG (or nematic state) with $w = 5$ meV, $T = 3$ K and (b) the doped, strained case with $w = 5$ meV, $T = 3$ K, and $\mu = 2$ and 6 meV. (c) The undoped gapped phase. (d) The unperturbed case with $\mu > 0$.

symmetry breaking in BLG using FIR spectroscopy through the weak absorption anisotropy of the strained/nematic state and the band-edge peak in the gapped state.

In conclusion, we have shown that IR and FIR absorption spectroscopy can distinguish between the gapless anisotropic nematic (or strain-induced) and the isotropic gapped broken symmetry states of BLG. The former has a characteristic strong dependence on the orientation of the polarization of the incident radiation, such that in the IR frequency range, light polarized perpendicularly to the strain axis (or symmetry-breaking axis in the nematic phase) will be absorbed very strongly at $\omega \approx \gamma_1 + w$ in the undoped system, whereas light polarized parallel to this axis acquires a characteristic feature in absorption when the doping is such that $\mu > w$. There is also a weak polarization dependence for strained BLG in the FIR regime, with the parallel polarization being absorbed more strongly. In contrast, the isotropic gapped phases show no absorption anisotropy, but do have a qualitatively different line shape from both strained BLG and the unperturbed state at zero or finite doping.

[1] E. McCann and V. I. Fal'ko, Phys. Rev. Lett. **96**, 086805 (2006).

[2] D. S. L. Abergel and V. I. Fal'ko, Phys. Rev. B **75**, 155430 (2007).

[3] E. J. Nicol and J. P. Carbotte, Phys. Rev. B **77**, 155409 (2008).

[4] F. Wang, Y. Zhang, C. Tian, C. Girit, A. Zettl, M. Crommie, and Y. R. Shen, Science **320**, 206 (2008).

[5] T. Ohta, A. Bostwick, T. Seyller, K. Horn, and E. Rotenberg, Science **313**, 951 (2006).

[6] Y. Zhang, T.-T. Tang, C. Girit, Z. Hao, M. C. Martin, A. Zettl, M. F. Crommie, Y. R. Shen, and F. Wang, Nature (London) **459**, 820 (2009).

[7] K. F. Mak, C. H. Lui, J. Shan, and T. F. Heinz, Phys. Rev. Lett. **102**, 256405 (2009).

[8] A. B. Kuzmenko, I. Crassee, D. van der Marel, P. Blake, and K. S. Novoselov, Phys. Rev. B **80**, 165406 (2009).

[9] Z. Q. Li, E. A. Henriksen, Z. Jiang, Z. Hao, M. C. Martin, P. Kim, H. L. Stormer, and D. N. Basov, Phys. Rev. Lett. **102**, 037403 (2009).

[10] M. Mucha-Kruczyński, I. L. Aleiner, and V. I. Fal'ko, Phys. Rev. B **84**, 041404 (2011).

[11] V. M. Pereira, A. H. Castro Neto, and N. M. R. Peres, Phys. Rev. B **80**, 045401 (2009).

[12] P. Dietl, F. Piéchon, and G. Montambaux, Phys. Rev. Lett. **100**, 236405 (2008).

[13] J. Nilsson, A. H. Castro Neto, N. M. R. Peres, and F. Guinea, Phys. Rev. B **73**, 214418 (2006).

[14] F. Zhang, H. Min, M. Polini, and A. H. MacDonald, Phys. Rev. B **81**, 041402 (2010).

[15] R. Nandkishore and L. Levitov, Phys. Rev. B **82**, 115124 (2010).

[16] R. Nandkishore and L. Levitov, Phys. Rev. Lett. **104**, 156803 (2010).

[17] J. Jung, F. Zhang, and A. H. MacDonald, Phys. Rev. B **83**, 115408 (2011).

[18] F. Zhang, J. Jung, G. A. Fiete, Q. Niu, and A. H. MacDonald, Phys. Rev. Lett. **106**, 156801 (2011).

[19] H. Min, G. Borghi, M. Polini, and A. H. MacDonald, Phys. Rev. B **77**, 041407 (2008).

[20] M. Kharitonov, arXiv:1109.1553.

[21] O. Vafek, Phys. Rev. B **82**, 205106 (2010).

[22] O. Vafek and K. Yang, Phys. Rev. B **81**, 041401 (2010).

[23] Y. Lemonik, I. L. Aleiner, C. Toke, and V. I. Fal'ko, Phys. Rev. B **82**, 201408 (2010).

[24] Y. Lemonik, I. L. Aleiner, and V. I. Fal'ko, Phys. Rev. B **85**, 245451 (2012).

[25] A. S. Mayorov, D. C. Elias, M. Mucha-Kruczyński, R. V. Gorbachev, T. Tudorovskiy, A. Zhukov, S. V. Morozov, M. I. Katsnelson, V. I. Fal'ko, A. K. Geim, and K. S. Novoselov, Science **333**, 860 (2011).

[26] J. Martin, B. E. Feldman, R. T. Weitz, M. T. Allen, and A. Yacoby, Phys. Rev. Lett. **105**, 256806 (2010).

[27] J. Velasco Jr., L. Jing, W. Bao, Y. Lee, P. Kratz, V. Aji, M. Bockrath, C. N. Lau, C. Varma, R. Stillwell, D. Smirnov, F. Zhang, J. Jung, and A. H. MacDonald, Nat. Nano. **7**, 156 (2012).

[28] F. Freitag, J. Trbovic, M. Weiss, and C. Schönenberger, Phys. Rev. Lett. **108**, 076602 (2012).

[29] F. Guinea, M. I. Katsnelson, and A. K. Geim, Nat. Phys. **6**, 30 (2010).

[30] For strain (Ref. 10) $w = \gamma_3(\delta - \delta')(\frac{d \ln \gamma_3}{dR_{AB}} - \frac{d \ln \gamma_0}{dR_{AB}})$, where δ and δ' are eigenvalues of the strain tensor, and R_{AB} is the closest neighbor distance between carbon atoms in the monolayer.

[31] Since this divergence is created by the existence of parallel bands, it may be cut off by any additional perturbation which modifies the slope of one band with respect to the other. For example, the next-nearest-neighbor interlayer hops, the interlayer hops from dimerized to undimerized lattice sites, or a momentum dependence of γ_1 (and therefore of the effective mass) can all cause this effect.

[32] For doped BLG, there is a step at $\omega = \gamma_1 \pm 2\mu$ because, for $\gamma_1 < \omega < 2\mu$, the transitions between the split valence band and low-energy conduction band are Pauli blocked. There is also a very sharp spike caused by the transitions between the two parallel conduction bands (low-energy band and split band at γ_1) for $k < \sqrt{2m\mu}/\hbar$.

[33] A. B. Kuzmenko, E. van Heumen, D. van der Marel, P. Lerch, P. Blake, K. S. Novoselov, and A. K. Geim, Phys. Rev. B **79**, 115441 (2009).